Formal Modelling and Validation of Rate-Adaptive Pacemakers

Marta Kwiatkowska*, Harriet Lea-Banks†, Alexandru Mereacre*, Nicola Paoletti*
*Department of Computer Science, University of Oxford, UK, name.surname@cs.ox.ac.uk
†University of Southampton, UK, harrietlea@btinternet.com

***Abstract*—Rate-adaptive pacemakers make use of sensors in order to automatically adjust the pacing rate according to the metabolic needs of the patient, thus overcoming the limitation of fixed-rate pacemakers that cannot ensure an adequate heart beat in cases of varying physical, mental or emotional activity. This feature significantly improves the quality of life of patients with chronotropic incompetence, i.e. whose heart is unable to increase its rate as the activity increases.**

We develop a formal model of a rate-adaptive pacemaker based on hybrid automata that explicitly includes sensors for rate control. In particular, we model the VVIR pacemaker with a QT interval sensor, a highly specific metabolic sensor that can sense the exercise activity level, based on the fact that physical (and mental) stresses shorten the QT interval, in turn requiring an increased heart rate. We implement the QT interval sensor through a runtime ECG detection algorithm and validate our model with patient data, showing that the simulated VVIR pacemaker is able to successfully regulate a Bradycardia ECG signal and produce a correctly paced heart.

The validated rate-adaptive pacemaker is plugged into the model-based framework introduced in [8], which enables rigorous and quantitative verification of closed-loop patient-device systems described as hybrid automata, and supports multiple heart and pacemaker models in a modular way. We demonstrate the usefulness of the framework by performing *in silico* experiments to demonstrate the correct functioning of rate modulation under different activity levels. Our framework has the potential to reduce the need for exercise testing with real patients.

I. Introduction

Cardiac pacemakers have revolutionised everyday life for more than $40,000$ people in England. Having a pacemaker fitted is now the most common type of cardiac surgery performed in the UK. Recent advancements in pacemaker design mean that quality of life is significantly improved, successfully delivering the essential and regular electric impulses required by the heart to keep the body alive.

The cardiac pacemaker is a small electrical device that uses electrodes embedded into the heart tissue to stimulate specific parts of the organ with a voltage, causing a heartbeat. In this study the VVIR pacemaker (where the ventricle is sensed and paced, and the rate adapts according to the physical activity of the patient) will be simulated. Depending on the location and frequency of the stimulations, the pacemaker may increase, decrease or stabilise the heart rate. A particularly slow resting heart rate (less than 60 bpm) is known as bradycardia and a particularly fast resting heart rate (greater than 100 bpm) is known as tachycardia. However, even a normal heart will not pace at a constant rate all day. The effect of exercise on heart rate is common knowledge, but early pacemakers did not appreciate this and paced at a constant rate. Consequently, quality of life was poor for patients and exercise was impossible.

One of the first rate-adaptive pacemakers was patented in 1981 and implemented the *automatic threshold tracking* [6] algorithm. Since then a number of different methods have been developed for adapting the pacing rate, including body motion, minute ventilation and QT interval [3]. Designing cardiac pacemakers is a time-consuming process, which requires rigorous methodologies to guarantee their safety through providing software quality assurance for embedded software. The particular challenge of rate-adaptive pacemakers is the need to ensure the correct functioning of rate modulation under different activity levels, which is typically achieved through exercises with real patients.

In this paper, we develop a formal model of a rate-adaptive pacemaker based on hybrid automata that explicitly includes sensors for rate control. The developed pacemaker model serves as a plug-in for the model-based framework for quantitative verification of closed-loop patient-device systems introduced in [8]. The framework, developed in Simulink in modular fashion, supports multiple heart and pacemaker models based on timed and hybrid automata, and enables the automated verification of properties such as "the pacemaker can correct faulty heart by maintaining the rhythm of 60-120 beats per minute". This paper focuses on extending the framework through providing novel functionality of *in silico* experiments to analyse rate modulation under different activity levels, with the aim to reduce the need for exercise testing with real patients.

We focus here on the VVIR pacemaker with a QT interval sensor, a highly specific metabolic sensor that can sense the exercise activity level, but the framework is sufficiently general to admit other types of pacemakers. The QT sensor measures the time difference between the Q wave and the T wave in the electrocardiogram (ECG) (see Fig.1). The VVIR pacemaker utilises the fact that physical (and mental) stresses shorten the QT interval, in turn requiring an increased heart rate. We implement the QT interval sensor through a runtime ECG detection algorithm and validate our model with patient data. We show that the simulated VVIR pacemaker is able to successfully regulate a bradycardia ECG signal and produce a correctly paced heart for a range of *in silico* induced activity levels, and scenarios including both healthy and faulty heart, and young and old patients. This demonstrates the usefulness of the framework to pacemaker developers in providing safety

† Contributed to the work during an internship funded by the ERC Advanced Grant VERIWARE.

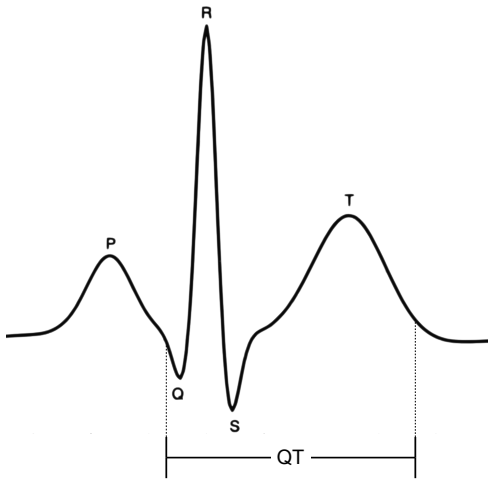

Fig. 1: Electrocardiogram.

assurance for their embedded software.

The specific contributions of this paper are:

- We develop a formal model of a VVIR pacemaker.
- We implement an ECG detection algorithm that models the functioning of the QT sensor.
- We perform extensive parametric analysis for identifying the parameter ranges that ensure the correct functioning of the pacemaker.
- We validate our modelling framework with real ECG data.

The paper is organized as follows. In Section II we present the results of the paper. In Section III we describe the modelling framework and also the ECG detection algorithm. In Section IV we give conclusions and discuss future work.

A. Related Work

Pacemaker software has been modelled and analysed using a number of approaches that employ formal methods. In [22], a dual-chamber pacemaker is modelled as a timed automaton, based on specifications provided by Boston Scientific, and verified using UPPAAL against a simple random heart model. Luu *et al.* [32] develop a real-time formal model for a pacemaker and verify it with the PAT model checker. Networks of timed automata are employed in the Virtual Heart Model [19]–[21], [29] and hybrid automata are used in the model of [4], [34], both analysed through simulation. Macedo *et al.* [26] develop and analyse a concurrent and distributed real-time model for pacemakers through a pragmatic incremental approach using VDM and scenarios. Gomes *et al.* [13] present a formal specification of the pacemaker using the Z notation and employ theorem proving, whereas Mert *et al.* [28] use Event-B and the ProB tool to validate their models.

Several works formulate heart models, but composition with pacemakers is not studied. In [14], [24], the authors develop a model of the cardiac conduction system that addresses the stochastic behaviour of the heart, validated via simulation. However, the hybrid behaviour of the heart is not considered. Grosu *et al.* [16] carry out automated formal analysis of a realistic cardiac cell model, and Grosu *et al.* [17] propose a method to learn and to detect the emergent behaviour (i.e. the spiral formation) that may lead to the onset of a ventricular fibrillation.

The modeling of the rate adaptive pacemaker has received limited attention in the verification community. In [31] and [28] the authors consider only the accelerometer-based pacemaker, just providing high-level specifications of the modulation mechanism. We instead develop concrete and executable models for both the QT sensor and the pacemaker component responsible for rate adaptation.

Related research also involves the definition of algorithms for the integration of signals coming from multiple sensors. Shin *et al.* develop a fuzzy algorithm that takes the inputs from the motion and the respiratory rate sensor in order to adapt the pacing rate to the physical activity of the patient. Amigoni *et al.* [2] use a multi agent-based cooperation mechanism to adapt the pacing rate of the patient based on the QT interval.

II. Results

We develop a formal model of a VVIR pacemaker and validate it on real patient data (see Sect. II-E). The pacemaker model is plugged into the model-based framework introduced in [8], which we enhance with the functionality to provide *in silico* experimentation aimed at demonstrating the correct functioning of rate modulation under different activity levels. We perform extensive parametric analyses (Sect. II-B) in order to study the behaviour of the pacemaker model under multiple QT interval (QTI) lengths and firing rates of the sinus node (SA node). This allows us to distinguish the parameter regions under which the pacemaker correctly operates from those where phenomena of sensor-induced tachycardia occur.

We model two different kinds of clinical conditions, corresponding to subjects with a healthy SA-node and with a form of chronotropic incompetence known as *Type II AV block* [11] (Sect. II-A), and we simulate the effects of an implanted pacemaker in both patients. Our results mainly focus on the latter class of patients, for which we show that any attempt to use a fixed-rate device fails in providing an adequate heart rate. In addition, we demonstrate the effectiveness of the derived rate-adaptive pacemaker model compared to the fixed-rate (VVI) pacemaker model over two scenarios: at a constant metabolic demand (Sect.II-C), where the VVIR model is proven to give robust responses to the detected QTIs; and by simulating the typical activity rates of both young and old patients during exercise (see Sect. II-D), which is commonly done in clinical practice to test and regulate pacemaker devices.

We used real ECG data from bradycardia patients both to derive a relationship, used in our VVIR implementation, between QTI length and heart rate by means of non-linear regression analysis; and to validate our VVIR model over real ECG signals (see Sect. II-E). We are able to show that our pacemaker implementation can correctly regulate not just sporadic bradyarrhythmia events, but also signals characterized by a constant low heart rate.

We implemented the VVIR pacemaker as a component of the model-based framework of [8], using Simulink and

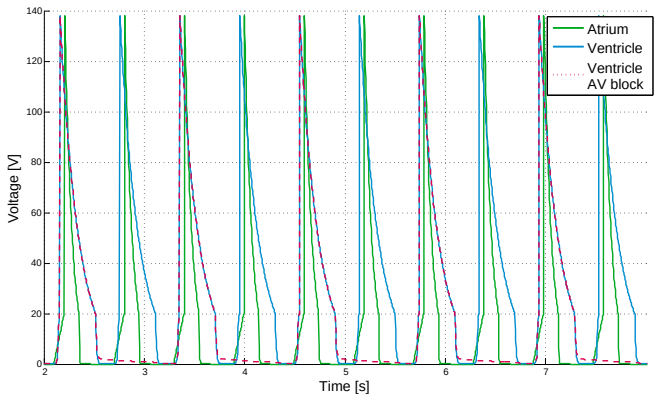

Fig. 2: Comparison of action potential curves in atrium (solid green line), in ventricle (solid blue line), and in ventricle under the simulation of a Type II AV block (dashed red line). In the latter case, only one half of the beats in the atrium (simulated at 100 BPM) reaches the ventricle.

a discrete-time simulation semantics. We considered a simulation step of 3.7 ms, yielding a path length of 16217 for a one-minute simulation, which is sufficient to capture the physiological behaviour of the heart. Every one-minute simulation took approximately 15 seconds on a 2.4 GHz Intel Core i5 CPU with 16GB of memory.

A. Simulation of AV block

Rate-adaptive pacemakers are mainly designed for patients with *chronotropic incompetence* [11], i.e. whose heart is unable to increase its rate as the intensity of activity increases. In order to test the effectiveness of our pacemaker model in this disease, we reproduce a so called *Type II AV block* [18], a defect in the atrioventricular node which intermittently fails to conduct P waves to the ventricle, resulting in a regular drop of ventricle beats. Figure 2 shows how the AV block affects the action potential in the ventricle. Results, obtained at a fixed rate of SA node stimulation of 100 BPM, highlight how the defective conduction leads to the loss of one half of the beats that would normally be delivered to the ventricle by a healthy AV node.

B. Parametric analysis under multiple QTIs

We perform extensive parametric analyses in order to study the behaviour of the pacemaker model under 23 different QTI lengths and 12 different firing rates of the SA node. In particular, we evaluate the total number of ventricular beats and the number of paced beats in one minute simulation, and compare the scenario of functional AV node against the Type II AV block. Even if the implantation of a pacemaker is clearly not necessary for a healthy individual, we are interested in testing our implementation under different sensor inputs, also in healthy conditions.

In our model, the length of a detected QTI directly affects the adaptive pacing rate, and specifically is used to compute the so-called *Lower Rate Interval* (TLRI), i.e. the pacemaker parameter indicating the longest period between two consecutive ventricular beats, used to impose the minimum heart rate. We consider the following law that relates QTI lengths and heart rate, suggested by Sarma et al. [30] in their re-evaluation of the standard Bazett's formula [5]:

$$\mathsf{RR}(\mathsf{QT}) = -\frac{\log\left((a-\mathsf{QT})/b\right)}{k} \tag{1}$$

where a, b and k have been estimated through non-linear regression as detailed in Sect. II-E; QT is the QTI length; and RR is the RR interval length (the distance between two R peaks, see Fig. 1), which expresses the heart rate and is used to update TLRI.

Results have been obtained after 552 simulations and are illustrated in Figure 3. The analysis of the total ventricular beats (V beats, Fig. 3 (a) and (b)) clearly shows a partition of the parameter space, approximately determined by the negative-slope diagonal crossing the x-y plane in the 3d plot. For each SA rate, this diagonal suggests an ideal lower bound for the QTI length.

Below this threshold, we observe quite an irregular pattern, characterized by a ventricular rate constantly higher than the SA rate, and such discrepancy is amplified as the QTI decreases. This behaviour can be classified as a *Sensor-Induced Tachycardia (SIT)* [7], [23], which generally occurs in adaptive pacemakers when the malfunctioning of the sensors leads to inappropriately fast pacing rate. In this case, the VVIR pacemaker wrongly detects a short QTI and adapts the pacing rate to values that are much higher than those needed by the actual demand (here determined by the SA node frequency). Hence, it fires an excessive number of paced beats to modulate the heart rate according to the (wrong) QTI. Indeed, we can observe the same partition of the parameter space in plots (c) and (d) of Fig. 3, showing the pacing frequency in the ventricle. Here, the region outlined by the QTI lengths below the ideal threshold is characterized by the highest pacing rates. Note that the erroneous behaviour of the pacemaker at short QTIs is mitigated in the AV block scenario, where the faulty AV node reduces the number of beats conducted to the ventricle, and thus the effect of sensor-induced tachycardia is less evident. In fact, the maximum ventricular rate is 164 BPM, obtained with a SA rate of 110 BPM and with the smallest QTI length considered (360 ms), while in the healthy case the extreme value is 202 BPM, with a SA rate of 120 BPM and QTI length of 360 ms.

On the other hand, if for each SA rate appropriate QTIs are considered (above the ideal lower bound), we observe a regular pattern in the number of ventricular beats. With a healthy AV node, they increase linearly in the number of SA beats, thus reproducing a correct conduction system which is not affected by wrong QTI detections. Contrarily, in the case of Type II AV block, the frequency in the ventricle grows linearly before reaching a final plateau, highlighting how, in a faulty conduction system, the number of lost beats increases with the SA rate. From Fig. 3 (c), we can further observe that, with appropriately detected QTI lengths and functional AV node, the VVIR pacemaker practically does not pace the ventricle at all, because of the correct functioning of the heart. On the other hand, as visible in plot (d), in the AV block scenario the pacemaker needs to provide additional beats in order to overcome the conduction defect, except for limited regions of

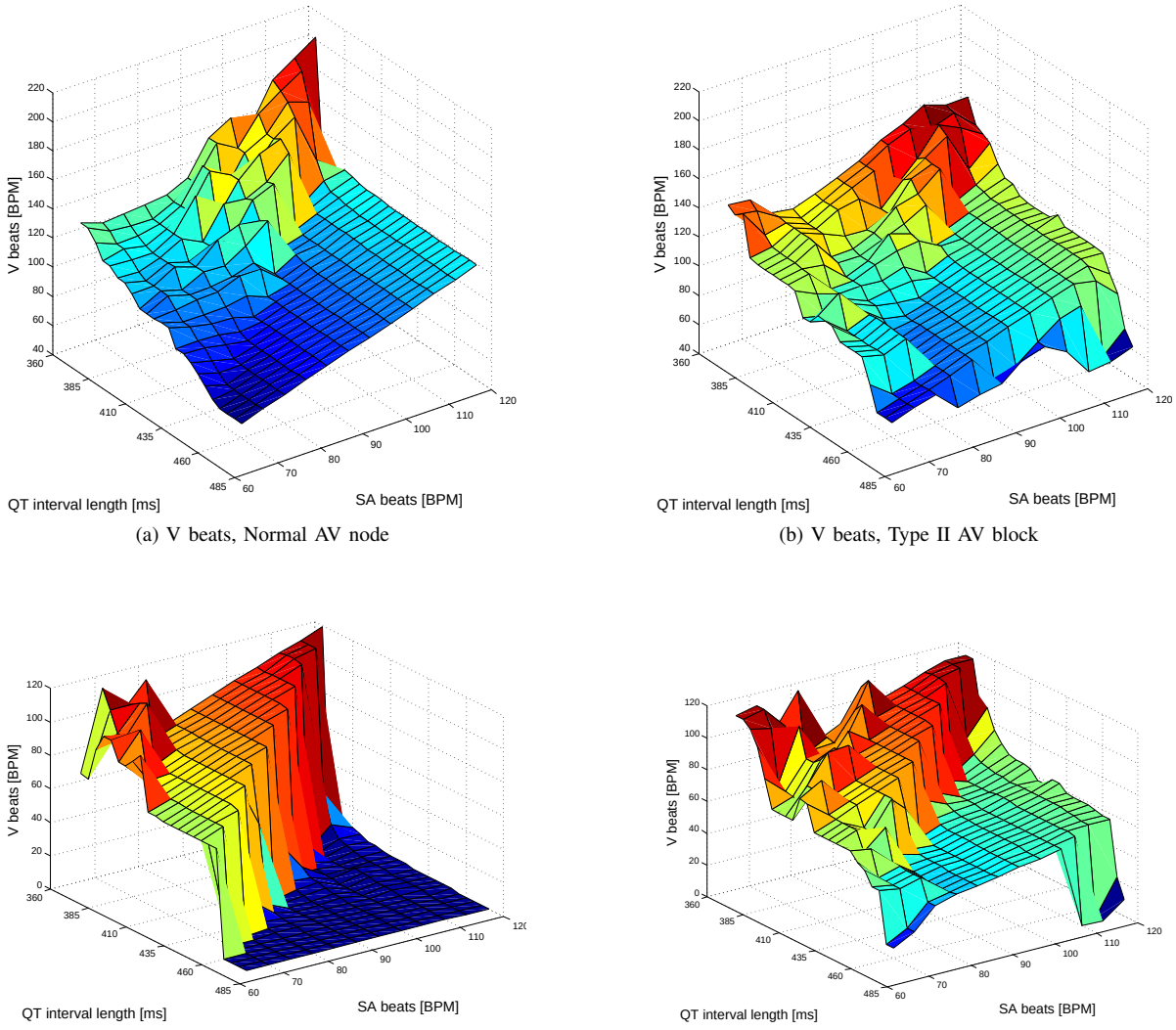

(a) V beats, Normal AV node

(b) V beats, Type II AV block

(c) Paced V beats, Normal AV node

(d) Paced V beats, Type II AV block

Fig. 3: Changes in the number of ventricular beats (z-axis) over multiple QTIs (x-axis) and SA node firing frequencies (y-axis). (a) and (c): simulation under normal AV conduction; (b) and (d): simulation under Type II AV block; (a) and (b): total number of ventricular beats; (c) and (d): number of paced beats.

the parameter space characterized by a low number of paced beats: with high SA frequencies and long QTI lengths, where the rate of conducted beats is anyway higher than the rate imposed by the corresponding TLRI; and with SA rates that are low enough to be successfully delivered to the ventricle with correctly detected QTIs.

For assessing the behaviour of the pacemaker device at fixed pacing rates, we analyse in Figure 4 individual contours of the above 3d plots, taken at fixed QTI lengths. In particular, we consider QTIs of 400, 430 and 460 ms, leading (according to Eq. 1) to TLRI values of 615, 758 and 1000 ms, in turn forcing a minimum heart rate of 97, 79 and 60 BPM respectively.

In Fig. 4 (a), we observe that, with a healthy AV node and long QTI, the ideal behaviour is obtained, for which the ventricular rate is the same as in the SA node. On the other hand, in the Type II AV block, the same QTI length cannot accommodate SA frequencies higher than 110 BPM, thus limiting the applicability of the corresponding TLRI during physical activity. As discussed before, the phenomenon of sensor-induced tachycardia occurs at SA rates lower than 80 BPM with a QTI length of 430 ms, and it is even more critical for a QTI of 400 ms where it can be observed for any SA frequency below 105 BPM. Besides leading to undesirable high rates, the TLRI resulting from the detection of short QTIs is still not enough to ensure an adequate number of ventricular beats in the AV block scenario (Fig. 4 (b)), where the maximum total number of beats is limited to 115 BPM.

Therefore, the conservative strategy of choosing long TLRIs (fixed, or as the result of long QTI detections) is more effective in both classes of patients. Indeed, the shorter the

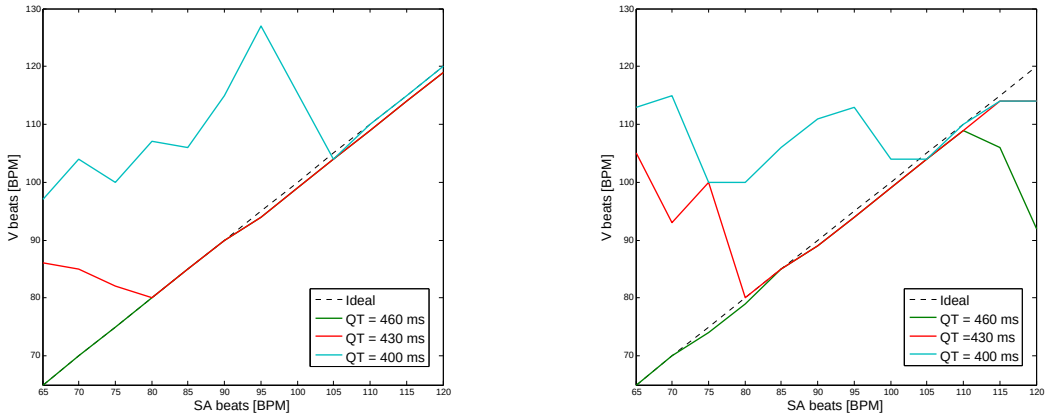

(a) Normal AV node

(b) Type II AV block

Fig. 4: Effects of fixed pacing rates with healthy AV node (a), and with AV block (b). The number of ventricular beats against different SA node frequencies are taken from Fig. 3 at fixed QTIs (400, 430 and 460 ms). The dashed black curves indicate the ideal behaviour with equal number of beats in the SA node and in the ventricle.

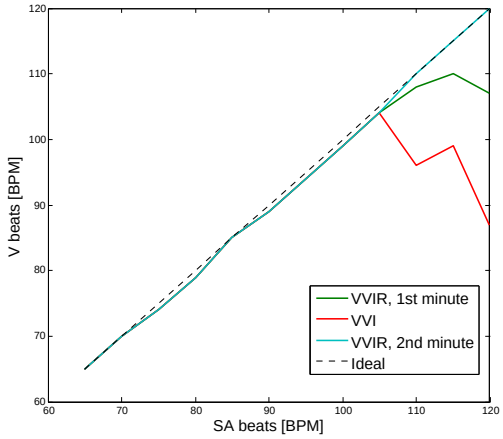

Fig. 5: Behaviour of the VVIR pacemaker compared to the fixed rate (TLRI $= 1000\ ms$) VVI pacemaker (red curve). The dashed curve shows the ideal behaviour of the conduction system. The number of beats in the ventricle in the first (green line) and in the second (blue line) minute of simulation with adaptive pacing are obtained at constant SA rate.

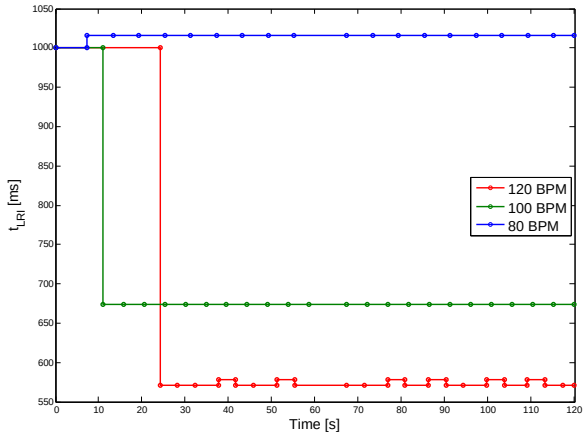

Fig. 6: Dynamics of rate modulation during a two-minutes simulation at constant SA rate of 80 (blue line), 100 (green) and 120 (red) BPM. Circles indicates time points where the TLRI is updated.

QTI length is, the wider is the range of SA frequencies under which we experience SIT. However, results clearly evidence that, with a faulty conduction system, there is no unique pacing rate able to deliver the correct number of beats to the ventricle for the considered spectrum of SA rates (65-120 BPM), and consequently for this class of patients the implantation of rate-modulated pacemakers appears mandatory.

C. Rate modulation under constant metabolic demand

We evaluate the performance of our implementation of VVIR pacemaker under the AV block scenario and when the heart is subject to a constant metabolic demand, here simulated through a constant SA rate. Figure 5 compares the behaviour of a fixed-rate VVI pacemaker (with TLRI set to the safe level of 1000 ms) against our VVIR pacemaker. In particular, we calculate the number of ventricle beats after one minute and two minutes of simulation at constant SA rate.

As previously discussed, we observe that the fixed-rate pacemaker is not able to deliver an adequately high number of beats at SA rates greater than 105 BPM. On the contrary, the VVIR pacemaker is clearly more effective in adapting the ventricular rate according to the actual demand. Specifically, after the first minute of simulation we record correct behaviour for SA frequency levels below 105 BPM. After this point, a slightly lower ventricular rate can be noticed, ranging in the interval 105-110 BPM for SA rates between 105-120 BPM.

This behaviour has to be attributed to the fact that the initial TLRI is set to the conservative level of 1000 ms, and thus, when the metabolic demand suddenly rises (i.e. high number of SA beats), the VVIR pacemaker needs more time to adapt to the correct pacing rate. Indeed, we observe that after the second minute of simulation at constant SA rate, the VVIR pacemaker is able to provide the correct number of ventricular beats.

Note that the adaptation delay during the first minute of simulation is a desirable feature in a rate-modulated pacemaker, because it provides a safer and more robust response to sudden metabolic increases, thus avoiding unnecessary overpacing in presence of too sensitive sensors [11].

The rate-modulation mechanism during a two-minute simulation is illustrated in Figure 6 for different fixed SA frequencies (80, 100 and 120 BPM) and starting from the same TLRI (1000 ms). Our implementation does not update the pacing rate at each QT detection, but it computes the TLRI over the average of the four last detections, in order to avoid stiff rate modulation dynamics that could occur with spurious QTIs. It is worth highlighting that, from the same (long) TLRI, the time needed for the first rate adaptation increases with the applied SA rate, evidencing the robustness of our VVIR model which "prudently" waits more time to change the pacing rate to a value much higher than the current one.

D. Rate modulation under physical activity

In this section, we aim to validate our VVIR pacemaker by simulating realistic exercise curves (taken from [9]). In healthy subjects, a fast heart rate increase is detected at the beginning of exercise (neural slope), followed by a slower increase (metabolic slope). Rate decay during recovery from exercise is generally fast after short exercise and prolonged after long and intense activity.

Here we reproduce and compare the typical physical activity curves of a young and old individual. In both classes of patients, the heart rate demand follows the above-described neural, metabolic and decay phases, but older subjects cannot provide the same exercise intensity as a young individual, and are consequently characterized by a lower maximum heart rate. Figure 7 shows the SA rates during 20 minutes exercise in young (plot (a)) and old (plot (b)) individuals, comparing the number of ventricular beats between the VVIR pacemaker and the fixed-rate VVI pacemaker. Again, we assume that both patients are affected by a faulty AV node and that the SA rate reflects the metabolic demand needed during the physical activity. Table I illustrates how exercise curves are constructed.

We report that our rate-adaptive pacemaker successfully manages to modulate the pacing rate according to the intensity of physical activity. Minor decreases in the ventricular frequency can be noticed only in correspondence of the most intense phases: in the young subject, at minutes 9, 10 and 11, the SA rate is 132, 136 and 140 BPM, while the number of V beats is 113, 117 and 134 BPM, respectively; in the old patient, at minute 11 the SA rate is 130 BPM, against a V rate of 114 BPM. However, such discrepancies are negligible if compared to the behaviour of the fixed rate pacemaker that is unable to provide an appropriate ventricular rate in response to SA rates higher than 110 BPM. Indeed, in the young subject, from minute 6 to 13, we register losses of ventricular beats between 31 and 43 BPM, while in the old one, fixed rate pacing leads to frequencies that are between 8 and 49 BPM lower than the SA rate (from minute 6 to 12). Even more importantly, we can observe that episodes of sensor-induced tachycardia never occur with the VVIR pacemaker, including at very high levels of physical activity.

	SA rate [BPM]	
	Young	**Old**
Neural slope ([0,5] min)	65 to 120	70 to 110
Metabolic slope ([5,10] min)	120 to 140	110 to 130
Decay ([10,15] min)	140 to 60	130 to 70
Resting ([15,20] min)	[60,75]	[70,75]

TABLE I: Simulated activity rates in young and old subjects during exercise. We assume a linear dynamics from the initial to the final rate of each phase, except from the resting phase, where the number of beats is randomly sampled from the reported discrete intervals.

E. Parameter estimation and validation with patient data

We validate our model with the ECG data of five patients, obtained from the PhysioNet database [12] (MIT-BIH Arrhythmia Database Directory and St. Petersburg Institute of Cardiological Technics 12-lead Arrhythmia Database). The considered subjects are reported to suffer from bradycardia arrhythmia, a condition of slow resting heart rate (typically lower than 60 BPM).

Since sequences of arrhythmias are sporadic, we firstly apply an RR interval detection algorithm in order to quickly identify sections of low heart rate within the 30 minute long ECG recordings. Secondly, we extract QTIs and RR intervals from the obtained bradycardia signals, by applying the ECG detection algorithm presented in Sect. III-D. Finally, we perform non-linear regression analysis over the sequences of computed QT and RR intervals according to the law proposed by Sarma et al. [30] and illustrated in Eq. 1 for relating QTI lengths and heart rate.

As detailed in [8], our model-based framework is able to simulate heart dynamics based on the generation of synthetic ECG signals, performed following [10], [27]. Here we extend the framework in order to compute ECG signals from prescribed sequences of QT and RR intervals. In this way, we were able to reproduce a heart behaviour based on the sequences of QT and RR intervals extracted from patient data through our detection algorithm.

We finally show the capability of our pacemaker implementation to regulate not just sporadic bradyarrhythmia events, but also signals characterized by a constant low heart rate. Figure 8 illustrate the results obtained by taking input SA node frequencies typical of bradycardia (between 40 and 60 BPM); a functional atrioventricular system; and multiple QTI lengths (454, 458, 462 and 466 ms) that are at the bordeline between

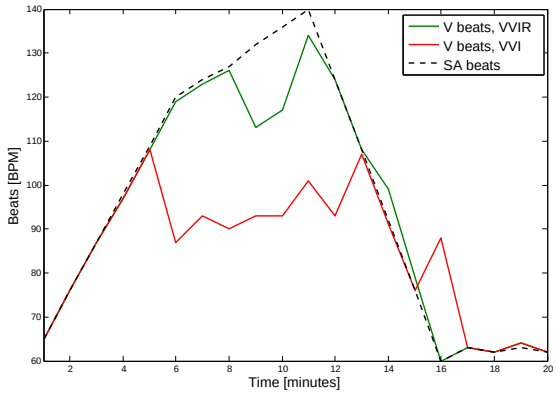

(a) Young patient

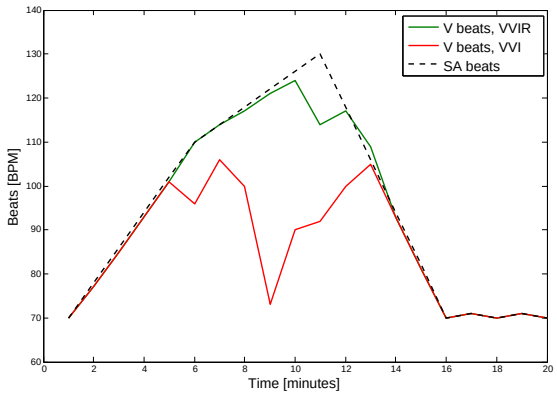

(b) Old patient

Fig. 7: Rate modulation during exercise in young (a) and old (b) patients. The SA rate (black dashed line) determines the metabolic demand during activity, and is calculated according to Table I. The number of ventricular beats is compared between the VVIR pacemaker (green curve) and the VVI pacemaker (red curve).

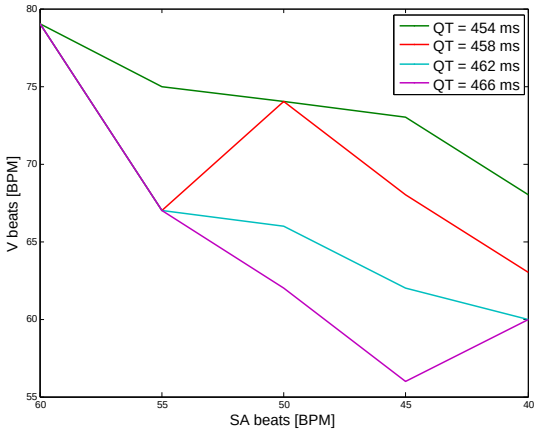

Fig. 8: Correction of bradycardia rythms by the VVIR pacemaker at different QTI lengths: 454 (green line), 458 (red), 462 (blue) and 466 (purple) ms. For the range of low SA rates (x-axis) considered (40-60 BPM), the number of V beats (y-axis) varies between 56 and 79 BPM.

normal and those reported in subjects with long QT syndrome [33]. Although the beats in the ventricle tend to decrease at lower SA rates and at longer QTIs, we can observe that the VVIR pacemaker is able to bring the ventricular rate to much safer levels, between 56 and 79 BPM.

III. Methods

We use hybrid input-output automata as a modelling framework for the pacemaker and the heart. First, we recall the model-based quantitative verification framework which was introduced in [8] and provide an example showing how one can model a single cardiac cell. Second, we provide an extension to the basic pacemaker specification by adding the rate adaptive component, which allows changing the pacing rate according to the physical activity of the patient. The rate adaptive component uses the QT sensor component to measure the time interval between the ventricular stimulus and the evoked T wave.

A. Hybrid automata model

In this section, we recall the basic details of the formal framework for the modelling and quantitative verification of pacemaker models that we introduced in [8]. The framework is based on hybrid input-output automata [25] and supports the composition of a heart model and a pacemaker model on which verification is performed.

Let $\mathcal{X} = \{x_1, \ldots, x_d\}$ be a set of variables in $\mathbb{R}$. An $\mathcal{X}$-valuation is a function $\eta : \mathcal{X} \to \mathbb{R}$ assigning to each variable $x \in \mathcal{X}$ a real value $\eta(x)$. Let $\mathcal{V}(\mathcal{X})$ denote the set of all valuations over $\mathcal{X}$. A *constraint* on $\mathcal{X}$, denoted by grd, is a conjunction of expressions of the form $x \bowtie c$ for variable $x \in \mathcal{X}$, comparison operator $\bowtie \in \{<, \leq, >, \geq\}$ and $c \in \mathbb{R}$. Let $\mathcal{B}(\mathcal{X})$ denote the set of constraints over $\mathcal{X}$. Let $\mathcal{Y}(\mathcal{X})$ denote the set of all real-valued functions over $2^{\mathcal{X}}$. We define $\mathcal{L}(\mathcal{X}) := \{x := u \mid x \in \mathcal{X} \wedge u \in \mathcal{X} \cup \{0\}\}$ to be the set of *update* assignments over the set of variables $\mathcal{X}$.

Definition 3.1 (Hybrid I/O Automaton): A hybrid I/O automaton (HIOA) $\mathcal{A} = (\mathcal{X}, Q, q_0, E_1, E_2, \mathrm{Inv}, \rightarrow, \mathrm{Diff})$ consists of:

- a finite set of variables $\mathcal{X}$;
- a finite set of modes Q, with the initial mode $q_0 \in Q$;
- a finite set E_1 of *input* actions and a finite set E_2 of *output* actions with $\mathcal{E} = E_1 \cup E_2$;
- an invariant function $\mathrm{Inv} : Q \to \mathcal{B}(\mathcal{X})$;
- a transition relation $\rightarrow \subseteq Q \times (\mathcal{E} \cup \{\varsigma\}) \times \mathcal{B}(\mathcal{X}) \times 2^{\mathcal{L}(\mathcal{X})} \times Q$, where ζ is the internal action; and
- a derivative function $\mathrm{Diff} : Q \times \mathcal{X} \to \mathcal{Y}(\mathcal{X})$ that assigns a function to a variable $x \in \mathcal{X}$.

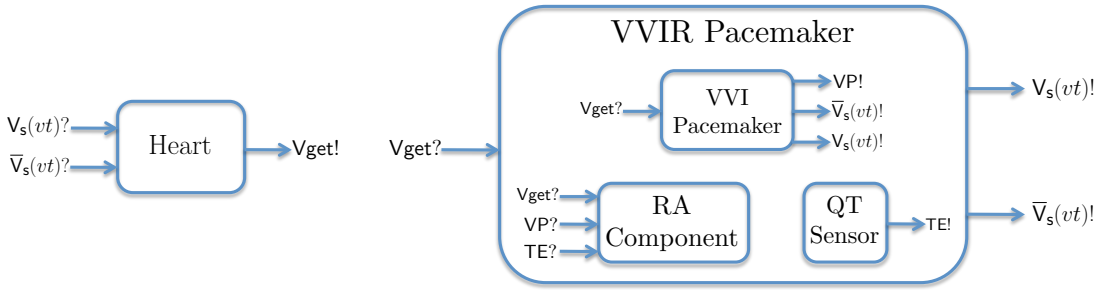

(a) Composition of the heart and VVIR pacemaker models

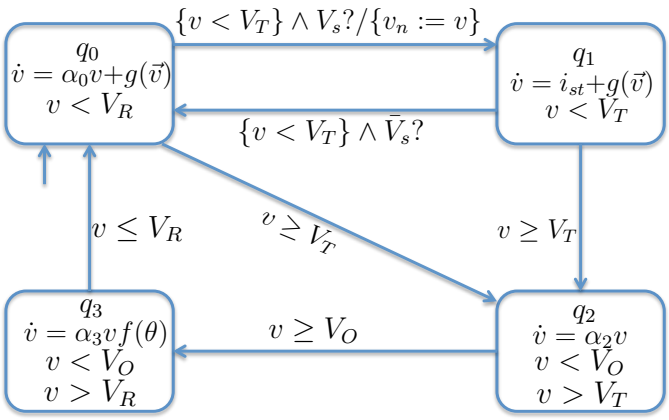

(b) Hybrid I/O automaton modelling a cardiac cell

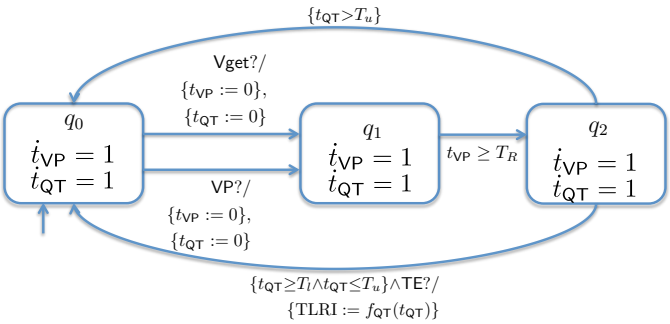

(c) Rate adaptive component

Fig. 9: Components of the modelling framework.

Example 3.1: In Fig.9(a) we depict a HIOA modelling a cardiac cell [34]. The HIOA consists of the set of variables $\mathcal{X} = \{v\}$, the set of locations $Q = \{q_0, q_1, q_2, q_3\}$, the set of input actions $E_1 = \{\mathsf{V}_s, \bar{\mathsf{V}}_s\}$ and the empty set of output actions. The variable v describes the value of the action potential in the cardiac cell. The set of input action denote the beginning and the end of the simulus event. The invariant for location q_0 is $v < V_R$ and the guard for the transition from location q_1 to location q_0 is $v < V_T$. The derivative function for variable v in location q_1 is $i_{\text{st}} + g(\vec{v})$. The dynamics in locations q_1 describes the behavior of the action potential under an external stimulus current i_{st} or the action potential of neighbouring cells.

B. Basic pacemaker components

The pacemaker is implanted under the chest skin and sends impulses to the heart at specific time intervals. In most cases the pacemaker comes implanted with two leads: one for the atrium and one for the ventricle. Each lead has the ability to sense or deliver an electrical signal. Here we extend the pacemaker model [22] based on Timed Automata (TAs) which was used to validate the framework from [8].

The pacemaker model in [22] consists of five basic TA components and an additional component that implements the rate adaptive (RA) algorithm. The basic components are: the lower rate interval (LRI) component, the atrio-ventricular interval (AVI) component, the upper rate interval (URI) component, the post ventricular atrial refractory period (PVARP) component and the ventricular refractory period (VRP) component. The LRI component has the function of keeping the heart rate above a given minimum value. The AVI component has the purpose to maintain the synchronisation between the atrial and the ventricular events. An event is when the pacemaker senses or generates an action. The AVI component also defines the longest interval between an atrial event and a ventricular event. The PVARP component notifies all other components that an atrial event has occurred. The URI component sets a lower bound on the times between consecutive ventricular events. The VRP component filters noise and early events that may cause undesired behaviour. The basic model described above represents the DDD type of pacemakers (sensing and pacing in both atrium and the ventricle). In this work we model the VVIR pacemaker, obtained from the basic model by including only sensing and pacing in the ventricle.

The components of the VVIR model and the interfaces with the heart model are depicted in Figure 9**??**. The sensing of a ventricular beat is implemented through action Vget, which notifies the pacemaker when there is an action potential from the ventricle. This signal is captured by the pacemaker only if the value of the action potential sensed from the ventricle crosses a given threshold. The output action VP notifies the pacemaker to pace the ventricle, while actions $\mathsf{V}_s(vt)$ and $\overline{\mathsf{V}_s}(vt)$ communicate the beginning and the end, respectively, of a paced ventricular impulse to the heart model. The VP event is generated by the VVI pacemaker component and is used to synchronize both the beginning of the paced impulse and the rate-adaptive (RA) component.

C. Rate adaptive component

The RA component is connected to the basic five pacemaker components in order to change the pacing rate according to the exercise activity of the patient. The pacing rate TLRI is set by the LRI component of the pacemaker model. When the basic pacemaker components function by themselves the value of TLRI remains fixed.

The task of the RA component is to change the value of TLRI according to the data received from the QT sensor component. In Simulink, we implement the QT sensor component as an ECG detection algorithm (see Section III-D). The output of the algorithm is the event TE!, which notifies the RA component of the exact time location of the T wave. In Figure 9(b) we depict the RA component as a HIOA.

In the initial state q_0, the RA component is always waiting for a ventricle sense event from atrium, Vget, or for a ventricle pace event, VP. When one of these events is enabled, the RA component starts two timers t_{VP} and t_{QT}. t_{VP} defines the refractory window of size T_R where the RA component disables the pacemaker inputs. t_{QT} defines the window where the RA component waits for the TE! event. If the TE! event arrives in the interval of time $[T^l, T^u]$ then the value of the QT interval is t_{QT}. This value is given as input to the function f_{QT} in order to compute the next pacing rate TLRI. The function f_{QT} reads from memory four previous stored QT values, takes the average and applies Eq.1 to get a new value for TLRI.

D. ECG detection algorithm.

In previous section we have described the rate adaptive pacemaker component which requires as input the TE event. In this section we present an implementation of the ECG detection algorithm that is used to detect each characteristic peak that defines the QTI length in the ECG signal. The sequencing and structure of the algorithm is based on [35]. The main task of the algorithm is to detect the R peak (see Fig.1) the most prominent peak in the ECG signal. This is achieved by pre-processing, applying the difference operation and finally detecting whether the value of the obtained signal crosses a given threshold.

Pre-processing of the ECG signal requires normalising (to ensure a 0 mV baseline) and filtering (to remove noise and baseline drift). The ECG signal is segmented into pre-defined time windows in order to analyse the QRS complex. The difference signal, as described in [35], uses the differential form $x_d(n) = x(n) - x(n-1)$, where $x(n)$ is the value of the ECG signal at step n. Once applied, this function generates the derivative ECG signal. The obtained signal is then separated into positive and negative halves.

To locate the R peak we find the turning point between each maxima in the positive difference signal and maxima in the negative difference signal. The point of zero gradient, in between these two maxima, indicates the location of the tip of the R peak. The location of the R peak is then used to locate the surrounding of the remaining points of interest - Q peak, S peak and T peak. The Q peak and S peak are both located using a search interval (in the x direction) relative to the R peak location and a magnitude threshold (in the y direction).

To calculate the T wave duration, we implement the method by Gritzali et al [15]. We define a search window alongside a magnitude threshold value. The Gritzali method then uses this threshold value to determine points of intersection with the ECG signal.

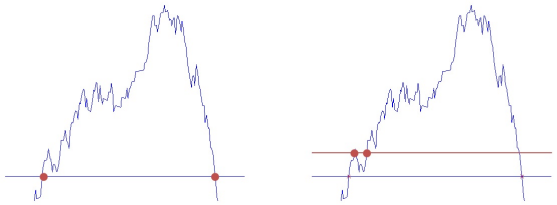

Fig. 10: Gritzali method for defining wave duration

However, when the signal is jagged the threshold can intersect the signal multiple times on a single side of the wave (see Fig.10). To overcome this issue we place several conditions on the selection of the intersection points and we use the peak of the wave as a reference point - always ensuring that one intersection point was on the left of the centre and another on the right. Once we compute the initial reference points we are able to determine the T wave duration and the QTI. The implemented algorithms require ECG data that is collected in advance. However, the algorithms can be modified to work in real time.

IV. Conclusion and Future Work

We have enhanced the model-based framework of [8] with the functionality to rigorously analyse the rate modulation capability of a rate-adaptive VVIR pacemaker under a variety of activity levels and patient types. We have implemented the QT sensor and validated our Simulink implementation on real patient data by demonstrating *in silico* that it corrects faulty heart behaviours. Our framework can help reduce the cost of pacemaker development by reducing the need for tests on real patients.

As future work, we plan to increase the physiological accuracy of the simulation, and implement a more complex heart model. Another natural step would be to extend the pacemaker specification and to include input from multiple sensors, such as motion and vibration. We also plan to exploit our framework to verify more advanced properties that could ensure the correct functioning of the enhanced pacemaker. Formal verification would provide a benchmark for proving and/or comparing the safety of such medical devices.

Acknowledgment

This work is supported by the ERC AdG VERIWARE, ERC PoC VERIPACE and the Institute for the Future of Computing, Oxford Martin School.

References

[1] PhysioNet. http://http://www.physionet.org/physiobank/.

[2] F. Amigoni, A. Beda, and N. Gatti. Combining rate-adaptive cardiac pacing algorithms via multiagent negotiation. *Information Technology in Biomedicine, IEEE Transactions on*, 10(1):11–18, 2006.

[3] S. S. Barold, R. X. Stroobandt, and A. F. Sinnaeve. *Cardiac pacemakers and resynchronization step by step: An illustrated guide*. John Wiley & Sons, 2010.

[4] E. Bartocci, F. Corradini, M. R. Di Berardini, E. Entcheva, S. A. Smolka, and R. Grosu. Modeling and simulation of cardiac tissue using hybrid i/o automata. *Theoretical Computer Science*, 410(33):3149–3165, 2009.

[5] H. Bazett. An analysis of the time-relations of electrocardiograms. *Heart*, 7:353–370, 1920.

[6] H. L. Brouwer, K. A. Mensink, and F. H. Wittkampf. Rate adaptive pacemaker and method of cardiac pacing, Dec. 15 1981. US Patent 4,305,396.

[7] T. Y. Cardall, W. J. Brady, T. C. Chan, J. C. Perry, G. M. Vilke, and P. Rosen. Permanent cardiac pacemakers: issues relevant to the emergency physician, part II. *The Journal of emergency medicine*, 17(4):697–709, 1999.

[8] T. Chen, M. Diciolla, M. Kwiatkowska, and A. Mereacre. Quantitative verification of implantable cardiac pacemakers over hybrid heart models. *Information and Computation*, In press, 2014.

[9] J. Clémenty, S. S. Barold, S. Garrigue, D. C. Shah, P. Jaıs, P. Le Métayer, and M. Haıssaguerre. Clinical significance of multiple sensor options: rate response optimization, sensor blending, and trending. *The American journal of cardiology*, 83(5):166–171, 1999.

[10] G. D. Clifford, S. Nemati, and R. Sameni. An artificial vector model for generating abnormal electrocardiographic rhythms. *Physiological measurement*, 31(5):595, 2010.

[11] S. Dell'Orto, P. Valli, and E. M. Greco. Sensors for rate responsive pacing. *Indian pacing and electrophysiology journal*, 4(3):137, 2004.

[12] A. L. Goldberger, L. A. Amaral, L. Glass, J. M. Hausdorff, P. C. Ivanov, R. G. Mark, J. E. Mietus, G. B. Moody, C.-K. Peng, and H. E. Stanley. Physiobank, physiotoolkit, and physionet components of a new research resource for complex physiologic signals. *Circulation*, 101(23):e215–e220, 2000.

[13] A. O. Gomes and M. V. M. Oliveira. Formal specification of a cardiac pacing system. In *FM 2009: Formal Methods*, pages 692–707. Springer, 2009.

[14] S. Greenhut, J. Jenkins, and R. MacDonald. A stochastic network model of the interaction between cardiac rhythm and artificial pacemaker. *Biomedical Engineering, IEEE Transactions on*, 40(9):845–858, 1993.

[15] F. Gritzali, G. Frangakis, and G. Papakonstantinou. Detection of the *P* and *T* waves in an ECG. *Computers and Biomedical Research*, 22(1):83–91, 1989.

[16] R. Grosu, E. Bartocci, F. Corradini, E. Entcheva, S. A. Smolka, and A. Wasilewska. Learning and detecting emergent behavior in networks of cardiac myocytes. In *Hybrid Systems: Computation and Control*, pages 229–243. Springer, 2008.

[17] R. Grosu, G. Batt, F. H. Fenton, J. Glimm, C. Le Guernic, S. A. Smolka, and E. Bartocci. From cardiac cells to genetic regulatory networks. In *Computer Aided Verification*, pages 396–411. Springer, 2011.

[18] J. R. Hampton. *The ECG in practice*. Elsevier Health Sciences, 2013.

[19] E. Jee, S. Wang, J. K. Kim, J. Lee, O. Sokolsky, and I. Lee. A safety-assured development approach for real-time software. In *Embedded and Real-Time Computing Systems and Applications (RTCSA), 2010 IEEE 16th International Conference on*, pages 133–142. IEEE, 2010.

[20] Z. Jiang, M. Pajic, A. Connolly, S. Dixit, and R. Mangharam. Real-time heart model for implantable cardiac device validation and verification. In *ECRTS*, pages 239–248, 2010.

[21] Z. Jiang, M. Pajic, and R. Mangharam. Cyber–physical modeling of implantable cardiac medical devices. *Proceedings of the IEEE*, 100(1):122–137, 2012.

[22] Z. Jiang, M. Pajic, S. Moarref, R. Alur, and R. Mangharam. Modeling and verification of a dual chamber implantable pacemaker. In *TACAS*, pages 188–203, 2012.

[23] C.-P. LAU, Y.-T. TAI, P.-C. FONG, C.-H. CHENG, and F. L.-W. CHUNG. Pacemaker mediated tachycardias in single chamber rate responsive pacing. *Pacing and Clinical Electrophysiology*, 13(12):1575–1579, 1990.

[24] J. Lian, H. Krätschmer, D. Müssig, and L. Stotts. Open source modeling of heart rhythm and cardiac pacing. *Open Pacing Electrophysiol Ther J*, 3:4, 2010.

[25] N. Lynch, R. Segala, F. Vaandrager, and H. B. Weinberg. *Hybrid I/O automata*. Springer, 1996.

[26] H. D. Macedo, P. G. Larsen, and J. Fitzgerald. Incremental Development of a Distributed Real-Time Model of a Cardiac Pacing System Using VDM. In *Formal Methods*, page 181, 2008.

[27] P. E. McSharry, G. D. Clifford, L. Tarassenko, and L. A. Smith. A dynamical model for generating synthetic electrocardiogram signals. *Biomedical Engineering, IEEE Transactions on*, 50(3):289–294, 2003.

[28] D. Méry and N. K. Singh. Pacemaker's Functional Behaviors in Event-B. Rapport de recherche, 2009.

[29] M. Pajic, Z. Jiang, I. Lee, O. Sokolsky, and R. Mangharam. From verification to implementation: A model translation tool and a pacemaker case study. In *Real-Time and Embedded Technology and Applications Symposium (RTAS), 2012 IEEE 18th*, pages 173–184. IEEE, 2012.

[30] J. S. Sarma, R. J. Sarma, M. Bilitch, D. Katz, and S. L. Song. An exponential formula for heart rate dependence of QT interval during exercise and cardiac pacing in humans: reevaluation of Bazett's formula. *The American journal of cardiology*, 54(1):103–108, 1984.

[31] B. Scientific. Pacemaker system specification. *Boston Scientific*, 2007.

[32] L. A. Tuan, M. C. Zheng, and Q. T. Tho. Modeling and verification of safety critical systems: A case study on pacemaker. In *Secure Software Integration and Reliability Improvement (SSIRI), 2010 Fourth International Conference on*, pages 23–32. IEEE, 2010.

[33] S. Viskin. The QT interval: too long, too short or just right. *Heart Rhythm*, 6(5):711–715, 2009.

[34] P. Ye, E. Entcheva, R. Grosu, and S. A. Smolka. Efficient modeling of excitable cells using hybrid automata. In *Proc. of CMSB*, volume 5, pages 216–227, 2005.

[35] Y.-C. Yeh and W.-J. Wang. QRS complexes detection for ECG signal: The Difference Operation Method. *Computer methods and programs in biomedicine*, 91(3):245–254, 2008.